Separation of alkali metal cations by a supported liquid membrane (SLM) operating under electro dialysis (ED) conditions

Qian, Zexin; Miedema, Henk; Sahin, Sevil; de Smet, Louis C.P.M.; Sudhölter, Ernst J.R.

DOI
10.1016/j.desal.2020.114631

Publication date
2020

Document Version
Final published version

Published in
Desalination

Desalination 495 (2020) 114631

Contents lists available at ScienceDirect

Desalination

journal homepage: www.elsevier.com/locate/desal

Separation of alkali metal cations by a supported liquid membrane (SLM) operating under electro dialysis (ED) conditions

Zexin Qian[a,b,*], Henk Miedema[b], Sevil Sahin[c], Louis C.P.M. de Smet[b,c,**], Ernst J.R. Sudhölter[a]

[a] Department of Chemical Engineering, Delft University of Technology, Van der Maasweg 9, 2629 HZ Delft, the Netherlands
[b] Wetsus, European Centre of Excellence for Sustainable Water Technology, Oostergoweg 9, 8911 MA Leeuwarden, the Netherlands
[c] Department of Organic Chemistry, Wageningen University, Stippeneng 4, 6708 WE Wageningen, the Netherlands

GRAPHICAL ABSTRACT

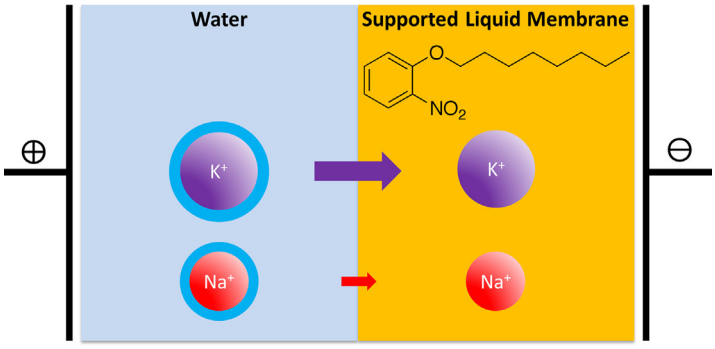

ARTICLE INFO

Keywords:
Supported liquid membrane
Alkali metal selectivity
K^+/Na^+ separation
Electro dialysis
Crown ether

ABSTRACT

This study demonstrates the effective separation of alkali metal cations using a Supported Liquid Membrane (SLM) containing lipophilic, negatively charged borate moieties, operating under electro dialysis conditions. The selectivity of the membrane is essentially based on differences in dehydration energy and mobility between ion species. The system favors the ion species with the largest crystal radius, despite its lower mobility. In mixtures of K^+ and Na^+, the SLM separates K^+ from Na^+ with a separation efficiency ranging from ~20% to 90%, depending on the feed solution composition. With solutions containing either K^+ or Na^+ and Li^+, the K^+/Na^+ over Li^+ separation efficiency is nearly 100%. Addition of 15-crown-5 derivative does not improve SLM behavior, but slows down the K^+ current by approximately 30% whereas the Na^+ current remains unaffected. As supported by simulations, the free K^+ and Na^+ ratio in the membrane (and with that the current ratio) is entirely defined by partitioning and the feed concentration ratio, regardless the presence of 15-crown-5. As a result, the current ratio of two ion species can be described exclusively in terms of their feed concentrations and crystal radii because the latter parameter defines both partitioning and mobility.

* Correspondence to: Z. Qian, Department of Chemical Engineering, Delft University of Technology, Van der Maasweg 9, 2629 HZ Delft, the Netherlands.
** Correspondence to: L. C.P.M. de Smet, Department of Organic Chemistry, Wageningen University, Stippeneng 4, 6708 WE Wageningen, the Netherlands.
E-mail addresses: zexin.qian@wetsus.nl (Z. Qian), louis.desmet@wur.nl (L.C.P.M. de Smet).

https://doi.org/10.1016/j.desal.2020.114631
Received 27 March 2020; Received in revised form 16 June 2020; Accepted 23 June 2020

1. Introduction

The underlying working mechanism of different types of membranes varies. The ability to discriminate between different components may be based on, for instance, charge, sieving, partitioning, mobility or the affinity between a guest and membrane-based host compound. In nanofiltration (NF) membranes, for instance, sieving properties dominate whereas in ion-exchange membranes (IEMs) charge is the predominant separation parameter. Most membranes exploit however a combination of two or more of these parameters. In IEMs, apart from charge, the interaction between a host and guest molecule as well as the mobility of the (partly dehydrated) ionic species may play a role.

The combination of IEMs with electro dialysis (ED) as applied in sea or waste water desalination has been widely reported [1–6]. There are two main reasons why this combination proved to be so fruitful. Firstly, transport enhancement by an electrical field is so much more efficient than a concentration gradient as driving force [7]. Secondly, currently existing IEMs possess a rather high selectivity in that they are quite well able to discriminate between cations and anions [8–10]. The fixed immobile charge inside the membrane effectively exclude co-ions (of the same sign of charge as the fixed charge inside), thereby preventing them entering the membrane. This concept, known as Donnan exclusion, works especially well as long as the concentration of co-ions in the surrounding solution is much lower than the fixed charges inside the membrane. The separation of two positively charged or two negatively charged ion species is also possible, at least if they differ in their valence, for instance, monovalent from divalent [11]. A membrane covered with, for instance, a positively charged top layer may repel divalent cations just strong enough, while meanwhile passing the monovalent cations [10]. It has been demonstrated that (co)polymer and nanofibers membranes can be used for the removal of Cu^{2+} ions from waste water [12–14].

A very challenging endeavor is the separation of two ionic species of the same charge, even more so if the two ion species are very similar in size. Once feasible, this possibility will open the way to novel applications in the field of selective element removal and element recovery, the former in the context of more severe legislation for discharge, the latter because of element scarcity. Because of its potential impact, the present study addresses this challenge. A previous study of this lab focused on the removal of Na^+ from the drainage water of greenhouses also containing K^+ [15]. Due to the salination of ground water and the fact that Na^+ is not taken up by plants, Na^+ accumulates in the (recycled) irrigation water. Whereas K^+ is an essential nutrient for plants, too high levels of Na^+ are toxic for most plants [16–18]. The challenge thus is to selectively remove Na^+ while leaving K^+ untouched as much as possible. Worth to mention is that the sensor community is familiar for decades already with artificial membranes capable of distinguishing between ionic species of the same charge. The (potentiometric) membranes of Ion Selective Electrodes (ISE) contain carrier molecules (*e.g.* crown ethers) with a high specific affinity for one particular ionic species [19,20]. A key difference between an ISE membrane and a typical separation membrane (the aim of the present study) is however that the fluxes over the ISE membrane are, or ideally should be, by definition essentially zero as any ion movement over the membrane will compromise the response sensitivity of the ISE.

The starting point of the present study is the so-called Supported Liquid Membrane or SLM. In short, in an SLM an organic phase is immobilized into an inert porous support, offering mechanical strength [21,22]. The SLM represents a three-phase extraction process where solutes can be extracted from one aqueous phase into another meanwhile passing the organic liquid phase in between. One reason to select the SLM as our membrane type of choice is the flexibility to add or adjust specific components to the organic phase [23]. The potential of SLM's in water desalination has been pointed out in [24]. Lipophilic salts have been widely reported to be used as ion exchanger in polymeric membranes for a good working performance [25–27]. Therefore, in order to improve its cation-over-anion selectivity and lower its ionic resistance, lipophilic anions are added to the SLM. These anionic sites are essentially the functional equivalent of the fixed permeant charge in typical ion-exchange membranes.

The present study reports on a SLM system implemented in an ED setting able to selectively enrich Na^+ from a solution also containing K^+. To generalize the concept of the SLM used, Li^+ is included in this study as well. Generally, SLM's contain specific carrier molecules to improve the membrane selectivity during the separation process [28–31]. For that reason, we explored the effect of inclusion of 15-crown-5 on SLM behavior. Finally, the application of the technology outlined here in green houses is briefly addressed including a test using a synthetic solution with the same composition as drainage irrigation water and a (brief) comment on the economic feasibility of the technology.

2. Materials and methods

2.1. Chemicals

All chemicals used were of analytical grade. The ACCUREL support (polypropylene, thickness: 100 μm, pore size: 0.1 μm) was purchased from MEMBRANA; the non-ionic base molecule for the synthesis of the lipophilic crown ether used as ion carrier, 2-hydroxymethyl-15-crown-5, from TCI Chemicals. All other chemicals were from Sigma-Aldrich: the organic solvent used for impregnating the ACCUREL support, 2-nitrophenyl-n-octyl ether (NPOE); the lipophilic backbone hydride-terminated poly(dimethylsiloxane), the catalyst chloride tris (triphenylphosphine)rhodium(I) (Wilkinson's catalyst); the solvent toluene (anhydrous); the lipophilic anion sodium tetrakis[3,5-bis(trifluoromethyl)phenyl]borate (NaBArF) and the salts, KCl, NaCl, LiCl and Na_2SO_4.

2.2. Crown ether synthesis

In order to prevent leaching out, 15-crown-5 was covalently attached to a rather bulky lipophilic backbone, *i.e.*, hydride-terminated poly(dimethylsiloxane) (PDMS), resulting in 1,8-(polydimethysily)propyloxymethyl-15-crown-5 (PSCE). Fig. 1 schematically shows the synthesis route of PSCE, a more detailed recipe and characterization can be found in the Supplementary Information.

2.3. Membrane preparation & stability

All experiments were performed with freshly prepared SLMs. The membrane support (ACCUREL) was submerged in the organic solvent mixture for 30 min, at RT. Due to capillary forces, the ACCUREL pores are filled up with solvent. Afterwards, excess solvent was removed by gently tissue wiping the membrane. The organic solvent mixture consisted of different combinations of NPOE, NaBArF and crown ether. If present, the NaBArF concentration always was fixed at 0.05 M. The crown ether concentration, as established by NMR, (see Supplementary Information), always was 0.13 M, a value close to its maximal solubility in NPOE [29].

As for membrane stability, the morphology of the membrane support and the obtained SLM before and after an ED experiment were assessed by SEM. No obvious changes were visible (see Supplementary Information).

2.4. Membrane characterization

2.4.1. Membrane selectivity

The membrane selectivity under zero-current conditions was assessed in a two-compartment measuring cell. For the cation over anion selectivity, one compartment was continually perfused with 0.5 M KCl solution, the other one with 0.005 M KCl. For the K^+ over Na^+

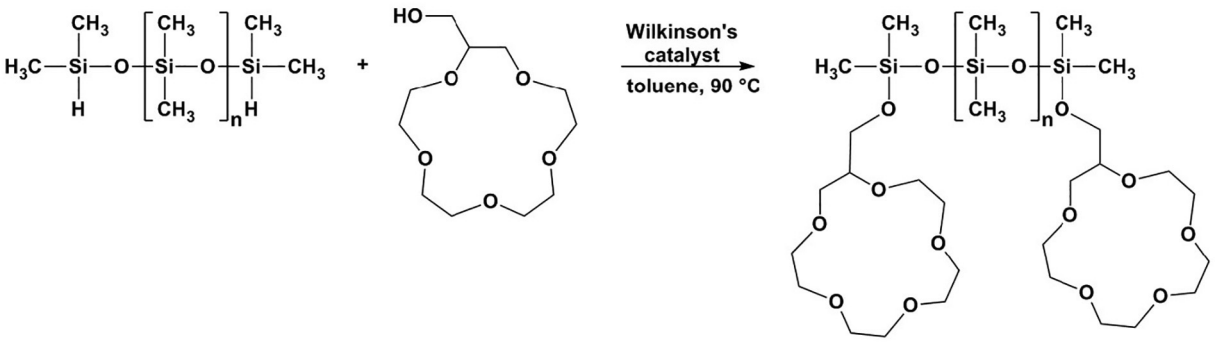

Fig. 1. Schematically depicted synthesis route of polysiloxane-bound crown ether (PSCE).

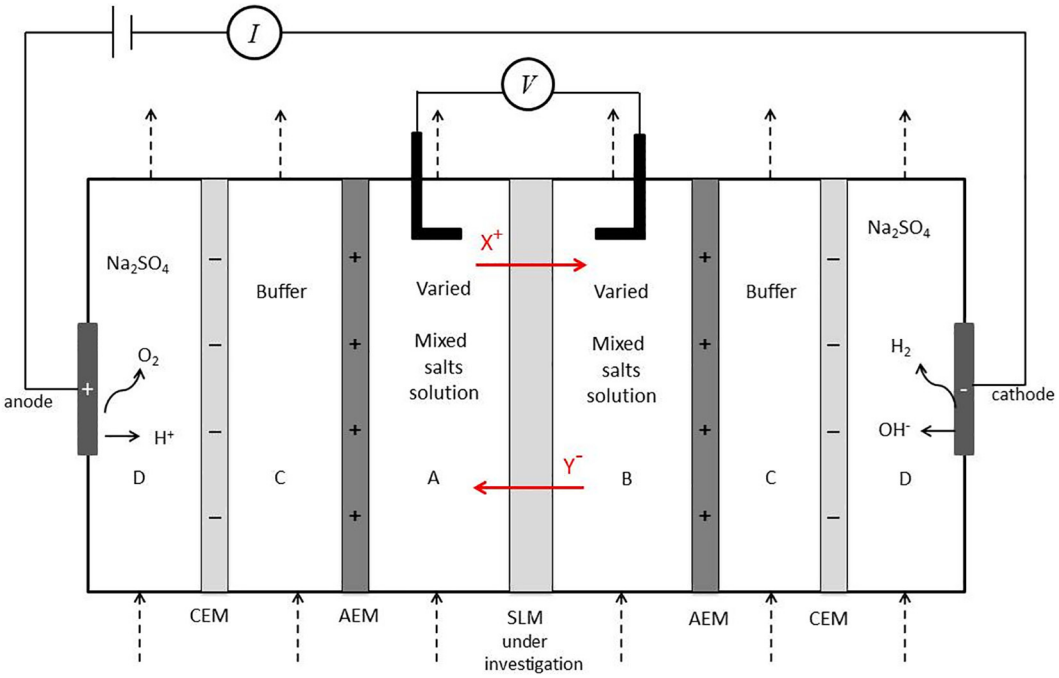

Fig. 2. Configuration of the six-compartment cell used during the electro dialysis experiments. Compartments C and D as well as the position of the CEM and AEM ensure that the concentration changes in the two inner measuring compartments arise solely from ion fluxes over the SLM.

selectivity, the SLM separated a 0.1 M KCl solution from a 0.1 M NaCl solution. Two double-junction Ag/AgCl reference electrodes recorded the potential difference over the SLM. The effective membrane surface area under investigation was 10.15 cm^2. All experiments were performed at room temperature (25 ± 0.2 °C. Following the protocol of Długołecki et al. [32], all membranes were conditioned in the solution of lower salt concentration (0.005 M KCl or 0.1 M NaCl solutions) for 24 h. Membrane potentials were measured 30 min after the start of perfusion the measuring cell with the proper solutions [32].

The reversal, equilibrium or zero-current potential (E_{rev}) of a membrane permeable for both monovalent cations and anions, *e.g.* K^+ and Cl^-, is given by the Goldman-Huxley-Katz or GHK equation:

$$E_{rev} = \frac{RT}{F} \ln \frac{P_K \times K_{feed} - P_{Cl} \times Cl_{receiving}}{P_K \times K_{receiving} - P_{Cl} \times Cl_{feed}} \quad (1)$$

R is the gas constant (8.314 $J\,K^{-1}\,mol^{-1}$), T is the temperature (K) and F is the Faraday constant (96,485C mol^{-1}), P_K and P_{Cl} are the permeability coefficient for K^+ and Cl^-, respectively, and with [K] and [Cl] in terms of activity rather than concentration.

Dividing the right term by P_{Cl} and after rearranging terms renders the expression for P_K/P_{Cl}:

$$\frac{P_K}{P_{Cl}} = \frac{\phi \times Cl_{feed} - Cl_{receiving}}{K_{feed} - \phi \times K_{receiving}} \quad (2)$$

with ϕ defined by:

$$\phi = \exp\left(\frac{FE_{rev}}{RT}\right) \quad (3)$$

For a membrane 100% selective for monovalent cations, *e.g.* K^+, Eq. (1) is reduced to the Nernst equation:

$$E_{rev} = E_N = \frac{RT}{F} \ln \frac{K_{feed}}{K_{receiving}} \quad (4)$$

The monovalent cation over monovalent cation selectivity, *e.g.* K^+ over Na^+, can be assessed under bi-ionic conditions with equimolar amounts of KCl and NaCl in the feed and receiving compartment, respectively [33,34]. Then, Eq. (1) reads:

$$E_{rev} = \frac{RT}{F} \ln \frac{P_K \times K_{feed}}{P_{Na} \times Na_{receiving}} \quad (5)$$

with the permeability ratio of P_K and P_{Na} given by:

$$\frac{P_K}{P_{Na}} = \phi \frac{[K]_{feed}}{[Na]_{receiving}} \quad (6)$$

Table 1
Crystal radii (in Å) of Li^+, Na^+ and K^+, as well as the Calculated Born ΔG (in kJ mol^{-1}) required for the transport of the particular ionic species from the aqueous into the NPOE/membrane phase. The value of α in the most-right column refers to Eq. (10).

	Crystal radius (in Å) [36,37]	ΔG (in kJ mol^{-1})	Ion pairs	α
Li^+	0.60	33.8	K^+/Na^+	11.7
Na^+	0.95	21.4	Na^+/Li^+	150.4
K^+	1.33	15.3	K^+/Li^+	1771.5

2.4.2. Electrodialysis (ED)

Apart from the behavior (selectivity) of the SLM under zero-current conditions, selectivity can be expressed in terms of transport numbers, a measure of the selectivity under non-zero current conditions and representing the current contribution of one particular ion species to the (forced) total current over the membrane. Ion transport across the SLMs was evaluated under ED conditions. Experiments were carried out in a six-compartment cell equipped with a platinum electrode (54 mm in diameter) in both outer compartments, as shown in Fig. 2. This way, possible redox reactions occurring in the two outer compartments do not affect the concentrations of the permeable ion species present in the two inner compartments directly facing the SLM. Also note the position of cation-exchange membranes (CEM from Neosepta) and anion-exchange membranes (AEM from Neosepta) separating the several compartments. In effect, changes in concentration in the two inner compartments can be attributed exclusively to ion transport over the SLM.

The effective surface area and thickness of the SLMs under investigation was 10.15 cm^2 and 100 μm, respectively. The feed compartment A and receiving compartment B were filled with (different) KCl or NaCl solution, depending on the type of selectivity assessed. Both C compartments were perfused with a recirculating buffer (1 L) solution with the same salt concentration as in A and B. The two outer D compartments recirculated an electrolyte solution containing 0.05 M Na_2SO_4 solution. Prior to use, SLMs were pre-conditioned for 24 h in the measuring solution of lowest salt concentration. Using a water bath, the temperature of all solutions was controlled at 25 ± 0.2 °C. A potentiostat (Ivium Technologies, Vertex. One, Eindhoven, The Netherlands) was employed as power source for applying a constant current (density). In order to monitor the voltage drop over the membrane, two Haber-Luggin capillaries were positioned directly adjacent to the SLM (Fig. 2) and connected to two reservoirs containing 3 M KCl-filled Ag/AgCl reference electrodes (QM711X, QIS, The Netherlands). Typically, a constant current of 10 mA (corresponding to a current density of 10 A m^{-2}) was applied during a time period of 24 (for single salt experiments) or 48 h (for all mixed salt experiments).

2.4.3. Transport numbers & mobility

Determination of transport numbers requires recording of the concentration changes in compartments A or B but preferably in both. Therefore, during the experiments every hour samples of 1 mL were taken from both compartments, with the ion concentrations determined by ion chromatography (IC, Metrohm Compact IC 761), at a confidence level > 95%.

The transport number t_i for monovalent ion species i is given by:

$$t_i = \frac{FV\frac{\Delta C}{\Delta t}}{I_{tot}A} \tag{7}$$

where V is the volume (L) of the feed and receiving compartment, A the effective membrane surface area (m^2), and I_{tot} the (constant) externally applied current density (A m^{-2}). The number of moles transferred over the SLM per unit time, $\Delta C/\Delta t$ (mol m^{-3} s^{-1}), was calculated from the change in concentration in both compartments A and B: $\Delta C = (C_{B,t} - C_{A,t}) / 2$ (mol m^{-3}).

During single-salt experiments (aiming to assess the ion mobility in the membrane), compartments A and B contained either symmetrical 0.1 M KCl, NaCl or LiCl. A constant (absolute) current of 10 A m^{-2} was applied during 24 h experimental time. The ion mobility u_i of ion species i is given by:

$$u_i = \frac{t_i I_{tot}}{c_i F\frac{E_m}{d}} \tag{8}$$

Here, c_i represents the free cation concentration in the membrane (in mol m^{-3}). Because of electro neutrality, c_i equals the concentration of immobilized lipophilic anions A in the membrane. Equating c_i with A presumes that ion pair formation between the free cations and A can be neglected. The electric field strength in the membrane (E_m/d) is defined as the ratio of recorded voltage drop over the SLM and its thickness (d).

2.4.4. Ion partitioning

The Born equation gives the ΔG of the transfer of an ion species of charge z and crystal radius r (in Å) from phase 1 with permittivity ε_1 to phase 2 with permittivity ε_2:

$$\Delta G = \frac{N_A z^2 e^2}{8\pi\varepsilon_0 r}\left(\frac{1}{\varepsilon_2} - \frac{1}{\varepsilon_1}\right) = \frac{695}{r}\left(\frac{1}{\varepsilon_2} - \frac{1}{\varepsilon_1}\right) = \frac{20.3}{r} \tag{9}$$

with ΔG in kJ mol^{-1}, N_A Avogadro's number (6.02×10^{23}), e the elementary charge (1.6022×10^{-19}C) and ε_0 the permittivity of vacuum (8.854×10^{-12} F m^{-1}). The pre-factors 695 and 20.3 in Eq. (9) result from transferring a monovalent cation ($z = 1$) from the aqueous ($\varepsilon_1 = 80$) into the NPOE/membrane phase ($\varepsilon_2 = 24$) [35].

Table 1 lists the crystal radii and the ΔG calculated according to the Born equation of the three monovalent cations used in this study.

The partitioning of both ion species over the (feed) aqueous and NPOE/membrane phase is defined by a Boltzmann distribution. In the case of K^+ and Na^+, the ratio of free K^+ and free Na^+ in the membrane, K_m/Na_m, equals:

$$\frac{K_m}{Na_m} = \frac{K_f}{Na_f}\exp\left(\frac{\Delta G_{Na} - \Delta G_K}{RT}\right) = \alpha\frac{[K]_f}{[Na]_f} \tag{10}$$

with $[K]_f$ and $[Na]_f$ the (time-dependent) K^+ and Na^+ concentration in the feed solution. After substituting the ΔG values for K^+ and Na^+ from Table 1, the numerical value of α turns out to be 11.7. For ion pairs Na^+/Li^+ and K^+/Li^+ the value of α equals 150.4 and 1771.5, respectively.

2.4.5. Membrane resistance

For the membrane resistance measurements, the configuration of the six-compartment cell as shown in Fig. 2 was slightly adapted in that all AEMs were replaced by CEMs. The SLM resistance was measured in (circulating) symmetrical 0.5 M NaCl solutions in compartments A and B. Prior to the actual recording, membranes were conditioned in 0.5 M NaCl solution for 24 h. All resistance measurements were performed at room temperature of 25 ± 0.2 °C. A potentiostat (Autolab AUT85567, The Netherlands) served as constant-current supply. The protocol followed was a step-wise increase of the current density, ranging from 0 to 2.5 A m^{-2}. The slope of the current density (A m^{-2}) *versus* voltage drop over the membrane (E_m) gives the (apparent) membrane resistance. The actual resistance of solely the SLM requires a resistance measurement of just the electrolyte solution as well. Subtraction of the latter from the former measurement renders the pure membrane resistance (Ω cm^2).

3. Results & discussion

3.1. Mass and charge balances

In order to investigate whether the ion concentration changes in the two inner compartments of the six-compartment cell in Fig. 2 can be exclusively ascribed to transport over the central membrane separating

Table 2
Mass and charge balance of compartments A and B, where charge balance refers to the net charge of the solution after accounting for the measured ion concentration changes. The third column, labelled Total, refers to the balances including all compartments A, B, C and D. Balances were calculated from measurements in either single-salt 0.1 M KCl and NaCl solutions or a mixed solution containing 0.05 M KCl and 0.05 M NaCl. N/A = Not Applicable.

	Single 0.1 M KCl			Single 0.1 M NaCl			Mixed 0.05 M KCl +0.05 M NaCl		
	A	B	Total	A	B	Total	A	B	Total
ΔK (mmol)	−0.17	0.16	−0.86	N/A	N/A	−0.01	−13.30	11.51	−1.18
ΔNa (mmol)	N/A	N/A	−0.33	−7.05	7.07	−0.02	−4.98	4.80	0.19
ΔCl (mmol)	−0.18	0.16	−1.20	−7.64	7.68	0.04	−17.15	15.16	−0.99
Δcharge (mmol e)	0.01	0	−0.01	0.56	−0.61	−0.01	−1.13	−1.15	0

chambers A and B, mass and charge balances were set up. Ideally, the changes of one particular ionic species in both compartments are the same but of opposite sign; stated otherwise, their summation adds up to zero. In addition, in order to retain electro neutrality, the total charge in each compartment also adds up to zero. As Table 2 shows, the mass and charge balance for both single and mixed salts solutions were indeed essentially closed. The same is true for the 'Total' balance taking into account all compartments. This bookkeeping gives credit to the concentration measurement of all ionic species involved by IC and ICP.

Careful analysis revealed that the discrepancy between the mass leaving the feed and entering the receiving phase as well as the non-zero total net charge are not due to ion accumulation inside the membrane. It is concluded that any deviation, *i.e.* non-zero value, falls in the error-range of ion concentration measurement by IC or ICP, typically ± 5%.

3.2. Membrane selectivity and membrane electrical resistance

First, the cation over anion selectivity of the SLM was assessed, as measured in asymmetrical 0.5/0.005 M KCl solutions, summarized in Table 3. With a P_K/P_{Cl} value of 357, the standard SLM, defined as a membrane containing both the solvent NPOE and lipophilic anion borate (A), clearly is cation selective in nature.

Taking out the lipophilic anion (SLM-A) turned the SLM in an essentially non-selective membrane, indicating that the observed K^+ over Cl^- selectivity of the SLM is solely due to the presence of A. Next we investigated the effect of the inclusion of polysiloxane bound 15-crown-5 (SLM + PSCE). Supplementing the SLM with PSCE drastically increased the selectivity to > 3000, almost a factor ten higher than the selectivity of the standard SLM. Even though this result may suggest a possible synergetic effect of A and PSCE, it should be realized that in this range, calculated permeability ratios are extremely sensitive to the measured reversal potential with large effects already upon shifts of merely a few mV's. The reason is both that the measured E_{rev} values asymptotically approach the theoretical Nernst potential of, in this case, K^+ (109 mV) and that the calculated P_K/P_{Cl} scales exponentially with E_{rev} (Eq. (2)). The P_K/P_{Cl} of a membrane containing PSCE but not A reduced to 12, emphasizing the predominant role of A in the cation over anion selectivity of the SLM with just a marginal contribution of PSCE, if any at all.

Table 3
Effect of excluding the lipophilic anion (A) or including the crown-ether (PSCE) on the K^+ over Cl^- selectivity, the K^+ over Na^+ selectivity and membrane resistance of the SLM.

	K^+ *vs.* Cl^- Selectivity	K^+ *vs.* Na^+ selectivity	Membrane resistance (Ω cm^{-2})
	P_K/P_{Cl}	P_K/P_{Na}	R
SLM (=NPOE + A)	357	30	440
SLM – A	0	19	12,142
SLM + PSCE	3069	59	3760
SLM + PSCE – A	12	76	4391

The next question concerned the membrane selectivity under bi-ionic conditions, with one chamber containing 0.1 M NaCl and the other 0.1 M KCl. As both solutions contain the common anion at the same concentration, any contribution of anion permeability to the recorded E_{rev} can be safely dismissed (Eq. (6)). Apart from the fact that all membranes tested clearly demonstrate K^+ over Na^+ selectivity, differences are less profound as seen in the charge selectivity previously discussed. With theoretical Nernst potentials of K^+ and Na^+ of $+/-\infty$, this observation also relates to the fact that measured E_{rev} values fall in a range where calculated P_K/P_{Na} values are relatively insensitive to E_{rev}. The picture that arises from the values of P_K/P_{Cl} and P_K/P_{Na} is that the lipophilic anion is responsible for the cation-over-anion selectivity, whereas the presence of PSCE only slightly improves the K^+ over Na^+ selectivity of the SLM. The slight improvement is possibly caused by the cation complexing properties of the PSCE and its higher affinity towards K^+.

The last column of Table 3 refers to the measured membrane resistance, as assessed in symmetrical 0.5 M NaCl. Most remarkable is the low resistance of the standard SLM and the high resistance of a membrane lacking the lipophilic anion A. Adding PSCE to the standard SLM increases the resistance nearly tenfold, an effect suggesting an interaction between the permeant cation and the hardly mobile PSCE, resulting in a lower mobility of the permeant cation.

3.3. Single-salt solutions: transfer numbers & mobility

Starting point are flux measurements in symmetrical 0.1 M KCl, NaCl or LiCl solutions over the SLM solely containing NPOE and A. Fig. 3 shows the normalized K^+, Na^+ and Li^+ concentration over time, *i.e.* the ratio of measured cation concentration and the initial cation concentration in feed compartment A (closed symbols). Note that in symmetrical solutions the minimum value of this normalized concentration is zero. For all three alkali metal ions, the relative cation concentration shows a similar linear decrease with time.

The transport numbers of K^+ and Na^+ (Eq. (7)) and the absolute amount of transported K^+ and Na^+ over the SLM can be derived from the data in Fig. 3. Once the transport number has been determined and together with the simultaneously recorded voltage drop over the SLM (E_m), the slope of Fig. 3 allows the calculation of the cation mobility (u) in the membrane, assuming that, due to overall electro neutrality, the free cation concentration in the membrane equals the concentration of lipophilic anion A (Eq. (8)). Table 4 summarizes the calculations based on data plotted in Fig. 3: ion transport number (t), membrane potential (E_m), absolute amount being transferred (in mmol) and ion mobility (u). Regarding the SLM data, the amount of salt transported as well as the transport number are very similar for K^+, Na^+ and Li^+, indicating that the current is predominantly cationic in nature, consistent with the high cation over anion selectivity of the SLM discussed in the previous

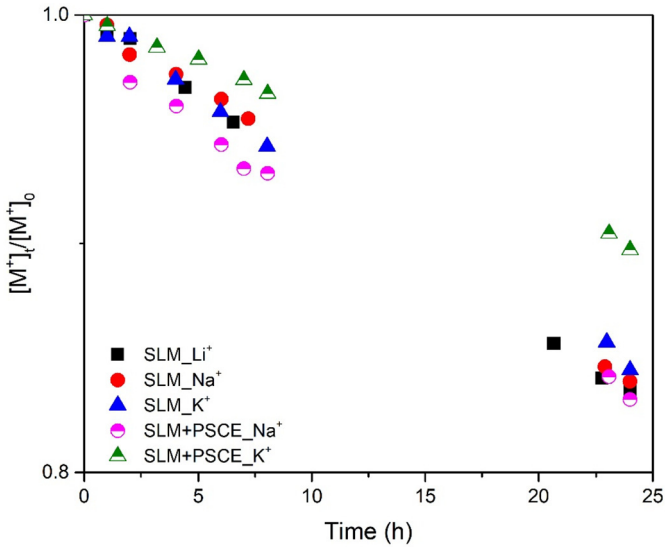

Fig. 3. Normalized K^+, Na^+ and Li^+ concentration in feed compartment A, recorded over time in symmetrical 0.1 M KCl, NaCl or LiCl solutions (closed symbols). Also shown, the effect of PSCE as determined in KCl and NaCl solutions (half open symbols).

Table 4
Transport numbers of K^+, Na^+ and Li^+ (t_{ion}), recorded membrane potential (E_m), absolute amount of transported cation from feed to receiving compartment and the ion mobility in the membrane (u_{ion}), all derived from single salt measurements.

0.1 M KCl	t_{ion}	E_m (V)	[K] (mmol)	$u_i \times 10^{-11}$ ($m^2\ V^{-1}\ s^{-1}$)
SLM	0.97	2.78	8.39	7.2
SLM + PSCE	0.73	1.01	6.03	5.4
0.1 M NaCl	t_{ion}	E_m (V)	[Na] (mmol)	$u_i \times 10^{-11}$ ($m^2\ V^{-1}\ s^{-1}$)
SLM	0.93	1.60	8.16	12.0
SLM + PSCE	0.96	1.89	8.43	12.4
0.1 M LiCl	t_{ion}	E_m (V)	[Li] (mmol)	$u_i \times 10^{-11}$ ($m^2\ V^{-1}\ s^{-1}$)
SLM	0.93	1.33	8.42	14.5

paragraph. Also note that the mobility of Na^+ and Li^+ are quite similar and significantly higher than the mobility of K^+. Even though the ion mobility is directly calculated from the recorded voltage drop over the membrane (Eq. (8)), the ratio of measured E_m (slightly) deviates from the reciprocal ratio of mobility values. For example, due to a small difference in transport number, the K^+/Na^+ E_m ratio of 2.78/1.6 = 1.74, is close but not identical to the Na^+/K^+ mobility ratio of 1.66.

Assuming that the ion can freely move within the SLM, the mobility of a completely dehydrated ion species is expected to be directly proportional to its reciprocal crystal radius. By approximation, this is indeed observed. First exemplified for K^+ and Na^+, the experimentally obtained Na^+/K^+ mobility ratio of 1.66 is indeed in reasonable agreement with the reciprocal ratio of their crystal radii of 1.4 (Table 1). For Li^+/Na^+ and Li^+/K^+ the measured mobility ratio is 1.21 and 2.09, respectively *versus* a reciprocal crystal radii ratio of 1.58 and 2.22, respectively. This observation supports the view that the charge carrier in the SLM is the dehydrated cation species, in agreement with the rather low permittivity of NPOE of 24. Small differences between the calculated mobility ratio and the reciprocal ratio of crystal radii may point to a possible (ion species-dependent) interaction between the permeant cation and the lipophilic anion.

3.4. Single-salt solutions: effect of crown ether

Next, the addition of PSCE on SLM behavior was investigated, corresponding to the SLM + PSCE data in Table 4 and the half open symbols in Fig. 3, showing how the presence of PSCE affects the K^+ concentration changes. The presence of PSCE clearly has a distinct effect when recorded in either K^+ or Na^+ solution. Whereas the K^+ transport number drops from 0.97 to 0.73 and the recorded E_m from 2.78 to 1.01 V, inclusion of PSCE hardly affects Na^+ transport, despite its recorded effect on E_m as listed in Table 3. This differential effect on K^+ and Na^+ transport indicates that K^+ (but not Na^+) interacts with the (rather immobile) PSCE, resulting in an overall reduced K^+ mobility. Note that the reduced E_m of 1.01 V in the presence of PSCE should not be interpret in terms of a reduced membrane resistance. The latter is defined by the slope of the IV-plot rather than the recorded voltage at one particular current density (as is the case here).

The reduced transport number of 0.73 raises the question about the identity of the ion species responsible for the remaining 0.27 part. Based on (changes in) measured pH values, H^+ as charge carrier can be excluded. The only candidate left is Cl^-, moving in opposite direction. Apparently, the constant applied current forces the SLM, despite its high cation selectivity, to the transport of Cl^-, all resulting from the reduced mobility of that part of K^+ interacting with PSCE and because transport numbers should add up to unity. The current carried by each ion species is directly proportional to both its concentration and its mobility in the membrane. As will be discussed in more detail later on, K^+ and Na^+ may interact with the lipophilic anion A. Because such interaction between Cl^- and A can be safely dismissed, the mobility of Cl^- might be (significantly) higher than the mobility of K^+ and Na^+. By implication, even though, in the case of KCl in the feed solution, Cl^- transport accounts for 27% of the total current, the actual number of Cl^- ions transported over the membrane might still be limited compared to that of K^+. Unfortunately, because of the configuration of the six-compartment cell with an AEM separating compartments A and B from C, quantifying the Cl^- current is impossible because of Cl^- entering from compartment C (Fig. 2). To compensate for the presence of Cl^- in the membrane, the actual K^+ concentration is expected to be (slightly) higher than the concentration in the absence of PSCE. Finally, the calculated mobility of K^+ in the presence of PSCE is an average value with contributions of both free K^+ and K^+/PSCE complex. Consistent with the conclusion that PSCE interacts with K^+, but not with Na^+, in K^+ this average value is lower than the value observed in a pure K^+ solution, whereas its value in a pure Na^+ solution remained unaffected.

3.5. Mixed salt solutions

Even though measurements in pure salt solutions, as described in the previous paragraph, may already point to a different SLM behavior in KCl and NaCl solutions, the selectivity observed in mixed salt solutions is essentially different in nature. Because the total number of cations cannot exceed the number of lipophilic anions, K^+ and Na^+ will actually compete to enter and/or move within the SLM. Therefore, transport studies were conducted in 1:1 solutions containing 0.05 M KCl and 0.05 M NaCl. Fig. 4a shows the measured (normalized) Na^+ and K^+ concentration in feed compartment A and ionic current over a time span of 48 h.

In 1:1 solutions (Fig. 4a), K^+ is transported right from the start with the K^+ carried current gradually decreasing over time. In contrast, initially Na^+ is hardly transported at all, but gradually increases over time with a stronger increase only after around 50% of the K^+ has already been removed from the feed solution. The initial Na^+ transport

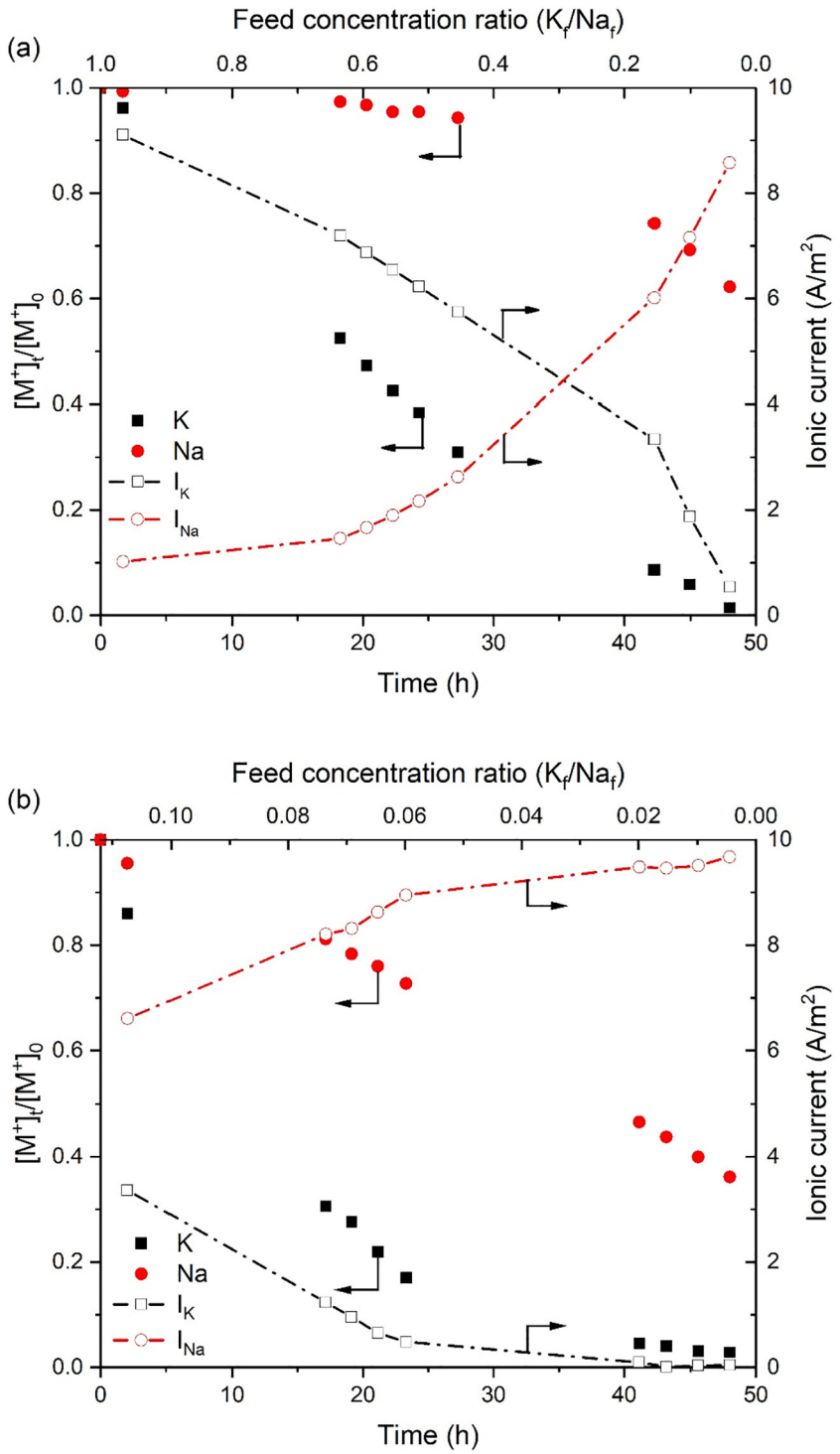

Fig. 4. Normalized K^+ and Na^+ concentrations and ionic current over time in symmetrical mixed salt solutions of either 0.05 M NaCl + 0.05 M KCl (a) or 0.09 M NaCl + 0.01 M KCL (b). Note that the top axis indicates the corresponding K^+ over Na^+ feed concentration ratio over time.

rate is forced to a higher level by increasing the (initial) Na^+/K^+ concentration ratio in the feed solution to 9:1, an effect shown in Fig. 4b. With 0.09 M NaCl and 0.01 M KCl present in the feed, Na^+ and K^+ transport start out simultaneously with the K^+ current decreasing and the Na^+ increasing over time. As evident from Fig. 4b, whereas the K current eventually completely vanishes, the Na^+ current reaches to near saturation level halfway the duration of the experiment. Apparently, with high Na^+ in the feed, the Na^+ level in the membrane reaches steady-state after about 25 h of forced ED. The summed transport numbers of K^+ and Na^+ calculated for the 1:1 and 9:1 mixed salt solutions are 0.97 and 0.92, respectively, indicating that also under these conditions the current is predominantly carried by cations.

3.6. Separation efficiency

Following Van der Bruggen et al. [38], the efficiency of the separation (S) of two components A and B (as function of time) is expressed by:

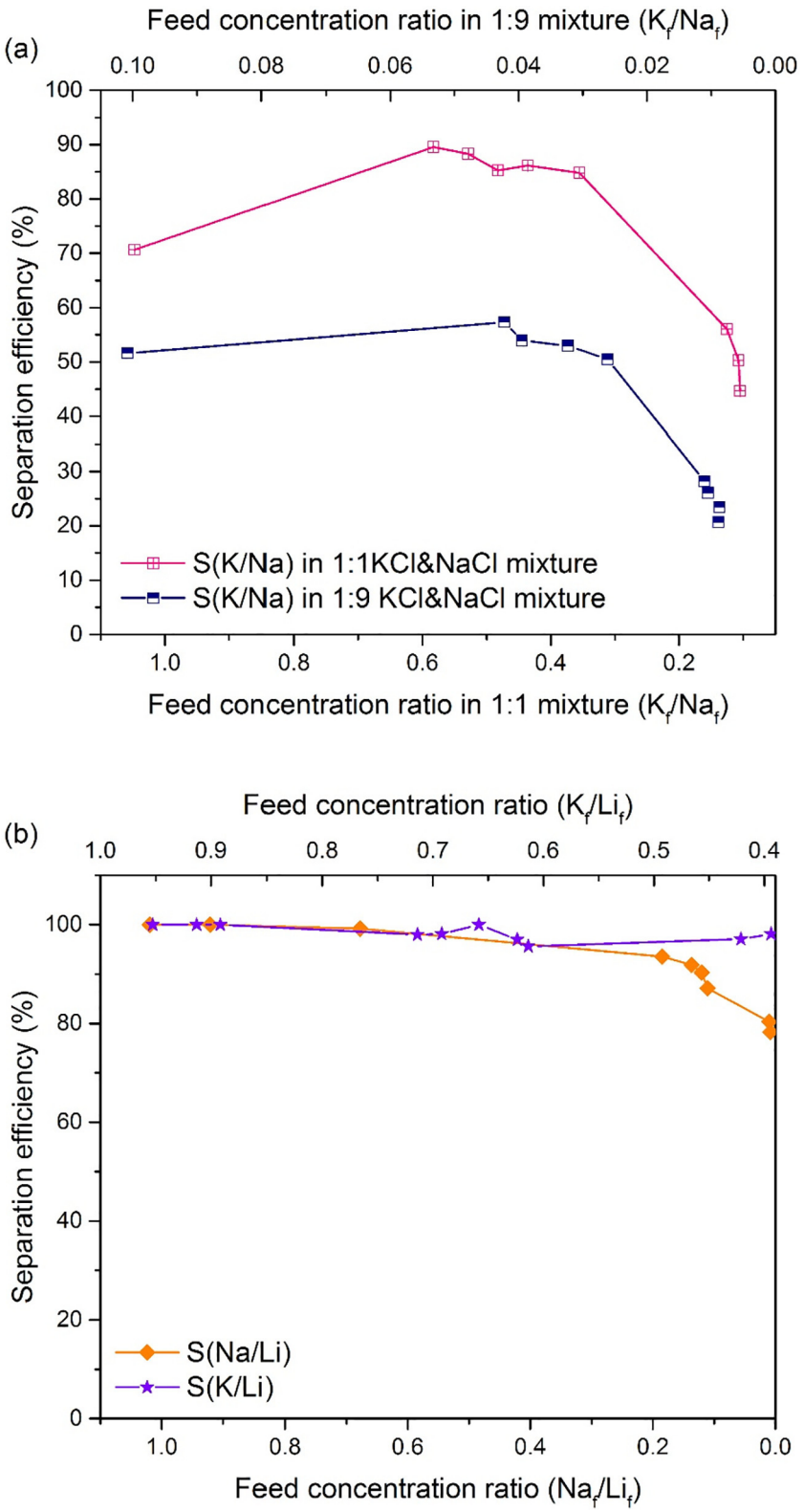

Fig. 5. Calculated separation factors derived from measurements in either symmetrical 1:1 (0.05 M NaCl + 0.05 M KCl) or 9:1 (0.09 M NaCl + 0.01 M KCL) solutions (a) or in symmetrical 1:1 (0.05 M NaCl + 0.05 M LiCl) or (0.05 M KCl + 0.05 M LiCl) solutions (b).

$$S(t) = \frac{[A]_t/[A]_0 - [B]_t/[B]_0}{(1 - [A]_t/[A]_0) + (1 - [B]_t/[B]_0)} \times 100\% \quad (11)$$

with $[A]_t$ and $[A]_0$ the concentration of component A in the dilute compartment (here the feed) at time t and time zero, respectively. Likewise for component B. In order to prevent calculating a value of $S(t) < 0$, Eq. (11) only holds in the case component A is the one species moving the slowest. Fig. 5a shows the separation factor S(K/Na) (is K^+ over Na^+ separation efficiency) as function of the normalized feed concentration ratio belonging to the data shown in Fig. 4. The initial rise from 70% to 90% for the 1:1 NaCl/KCl mixture and from 50% to

~55% for the 9:1 NaCl/KCl mixture, most likely reflects the exchange of Na^+ for K^+ because the membranes were equilibrated in NaCl. As expected, the K^+ over Na^+ separation efficiency decreases with increasing the feed Na^+/K^+ concentration ratio even though the shape of the two curves in 1:1 and 9:1 solutions are identical. Fig. 5b shows the separation efficiency data for mixed 1:1 salt solutions of NaCl/LiCl and KCl/LiCl. Compared to S(K/Na) show in Fig. 5a, both the Na^+ over Li^+, S(Na/Li), and K^+ over Li^+ separation efficiency, S(K/Li), are not only higher but remain over time near the 95–100% level with only S(Na/Li) dropping to 80% at Na/Li feed concentrations < 0.1.

3.7. Mechanism of selectivity

This paragraph explores the possible role of the (difference in) dehydration energy between two ion species in the observed selectivity of the SLM. As for K^+ and Na^+, the K^+/Na^+ current ratio (at any time) can be derived from Fig. 4 as the ratio of both normalized concentration *versus* time slope values. Starting from the general expression $I = zcuFE_m/d$ (with c the concentration of the particular ion species in the membrane), the current ratio of K^+ and Na^+ (I_K/I_{Na}) is directly proportional to the product of the mobility ratio of both ion species u_{Na}/u_K and the ratio of the K^+ and Na^+ concentration in the membrane. The former has already been obtained from the single-salt measurements (=1.66, see Table 4), rendering the membrane concentration ratio K_m/Na_m given by:

$$\frac{K_m}{Na_m} = \frac{u_{Na}}{u_K}\frac{I_K}{I_{Na}} = 1.66 \times \frac{I_K}{I_{Na}} \tag{12}$$

Eq. (12) gives the experimentally obtained value of K_m/Na_m as function of time in relation to the (time-dependent) value of I_K/I_{Na}. Eq. (10), on the other hand, predicts the theoretical value of K_m/Na_m. Fig. 6a plots the experimentally obtained value of K_m/Na_m *versus* the calculated theoretically predicted value, both as function of the time-dependent K_f/Na_f and starting in either 1:1 or 9:1 NaCl:KCl solutions. As visible guidance, the dotted line in Fig. 6 represents the line of equality with a slope of unity ($\alpha = 1$), *i.e.*, the ideal case in which experimental and predicted values are identical.

The slopes (α) experimentally obtained from linear fits (not shown) of the date sets of Fig. 6 are: 1.12 for 1:1 Na/K; 1.02 for 9:1 Na/K; 1.03 for Na/Li and 0.98 for K/Li. These values are close (enough) to the ideal case of $\alpha = 1$. This result justifies the conclusion that Fig. 6 provides evidence that the SLM has a preference for the ion species with the largest crystal radius, an effect due to the fact that a larger crystal radius pairs with a lower dehydration energy. The hypothesis that dehydration dictates the current ratio of the two ion species is supported by measurements in mixed salt solutions of either NaCl and LiCl or KCl and LiCl. Fig. 6b shows similar data as Fig. 6a but for 1:1 Na^+/Li^+ and K^+/Li^+ mixtures. Because of its crystal radius, Na^+ (0.95 Å) outcompetes the smaller Li^+ (0.60 Å) for exactly the same reason as K^+ (1.33 Å) is able to outcompete the smaller Na^+. Note the difference in range of membrane concentration ratio between panels (a) and (b) of Fig. 6. Including the Li^+ data of Fig. 6b extrapolates the validity of the argument to membrane concentration ratios up to a value of 150 for the Na/Li mixture to ~800–900 for the K/Li mixture (with a deviation of linearity at larger ratios).

In agreement with the above-mentioned observations, with a large difference in crystal radii of 0.73 Å, the separation efficiency shown in Fig. 5 is highest for K^+ and Li^+ compared to those recorded in either K^+/Na^+ or Na^+/Li^+ mixtures.

Combining Eqs. (9), (10) and (12) results in an expression of the current ratio exclusively in terms of the crystal radii of both ion species and the feed concentration ratio. For instance, the current ratio I_K/I_{Na} in the K^+/Na^+ solution is given by:

$$\frac{I_K}{I_{Na}} = \frac{r_{Na}}{r_K}\exp\left(\frac{20300}{RT}\left(\frac{1}{r_{Na}} - \frac{1}{r_K}\right)\right)\frac{K_f}{Na_f} = \beta\frac{K_f}{Na_f} \tag{13}$$

with β adopting the value of 8.4, implying that only at Na^+ concentrations in the feed exceeding the K^+ concentration by a factor 8.4, will the Na^+ flux be larger than the K^+ flux over the membrane. This is the reason that in symmetrical 1:1 solutions K^+ is the dominant ion species transported whereas in 9:1 mixtures the current is initially carried by both K^+ and Na^+. For ion combinations Na^+/Li^+ and K^+/Li^+, the value of β is 97.3 and 819.9, respectively. Eq. (13) predicts a linear relationship between the current ratio and the feed concentration ratio, which is indeed observed experimentally. Fig. 7 shows for all three ion combinations the measured current ratio as function of the (time-dependent) feed concentration ratio. The dotted lines in Fig. 7 are based on the theoretical β values and the current ratio predicted by Eq. (13). Any deviation between the experimental (actual regression lines not shown) and theoretical curves may relate to effects not taken into account by Eq. (13), for example, an interaction between the permeating cation and the lipophilic borate or an ion permeation mechanism requiring partial dehydration only, leading to an underestimation of the actual ion radius and hence overestimation of both its dehydration energy and mobility. However, despite the shortcomings of the very simplified view expressed by Eq. (13), as Fig. 7 shows, with increasing size difference between the two ion species (*e.g.* for K^+ and Li^+), ion radius starts to dominate SLM behavior.

Finally, a word on the difference between the selectivity measured under zero-current and bi-ionic conditions (Table 3) and the selectivity reflected by the current ratio as shown in Fig. 7. The K^+ over Na^+ selectivity of 30 shown in Table 3 is about three times the value of ~10 following from the ED measurement with equal feed concentrations, *i.e.* $K_f/Na_f = 1$ (Fig. 7a). Apart from differences in ionic conditions, one reason for the difference in selectivity may the role of mobility. Whereas this parameter plays no role in the equilibrium potential established during the zero-current measurement, during ED it works against the larger K^+, the ion species that is favored because of partitioning reasons. This effect may indeed lower the K^+ over Na^+ selectivity under ED conditions. The observation that different types of selectivity measurements may lead to a different outcome has also been reported by [34], in which selectivity determination by Donnan dialysis has been compared with an assessment by ED.

3.8. Interaction between K^+/Na^+ and CE

The idea behind adding a crown ether is that cation coordination by crown ether oxygens compensates for the energy penalty due to the required ion dehydration for entering the membrane. As a result, the CE enhances the partitioning of the particular ion species over the membrane phase. Given the cavity size of 15-crown-5, it was actually anticipated that 15-crown-5 would predominantly interact with Na^+ rather than with K^+ [39]. However, as shown in Fig. 3, addition of modified 15-crown-5 (PSCE) affects the transport of K^+ but not of Na^+. An explanation for the observed effect on the K^+ current is that (in this particular case) ring size is actually not the defining parameter because the ion is possibly sandwiched between two (or more) crown ether molecules due to the lower interaction energy compared the interaction energy with only a single crown involved [40–42]. Alternatively, 15-crown-5 may indeed show a higher affinity for Na^+ but this effect is obscured by the effect on the K^+ current because the latter ion species is present at a higher concentration, due to the favored partitioning discussed in previous paragraphs. It is this second possibility that will be explored here in more detail. Therefore, we modelled the interaction between CE and K^+/Na^+ using set values for the equilibrium affinity constants (K_K and K_{Na}) of the CE - metal ion complexes, CE-K and CE-Na. Let K_m and Na_m be the free K^+ and Na^+ concentration in the membrane, A the lipophilic anion concentration, CE_{tot} is the total CE concentration, being the sum of free CE, CE_0 (*i.e.* not complexed with K^+ or Na^+) and complexed CE-K and CE-Na. The following set of equations fully describes the system in terms of fixed total amount of CE (Eq. (14)), electro neutrality (Eq. (15)), affinity constants of CE for K^+

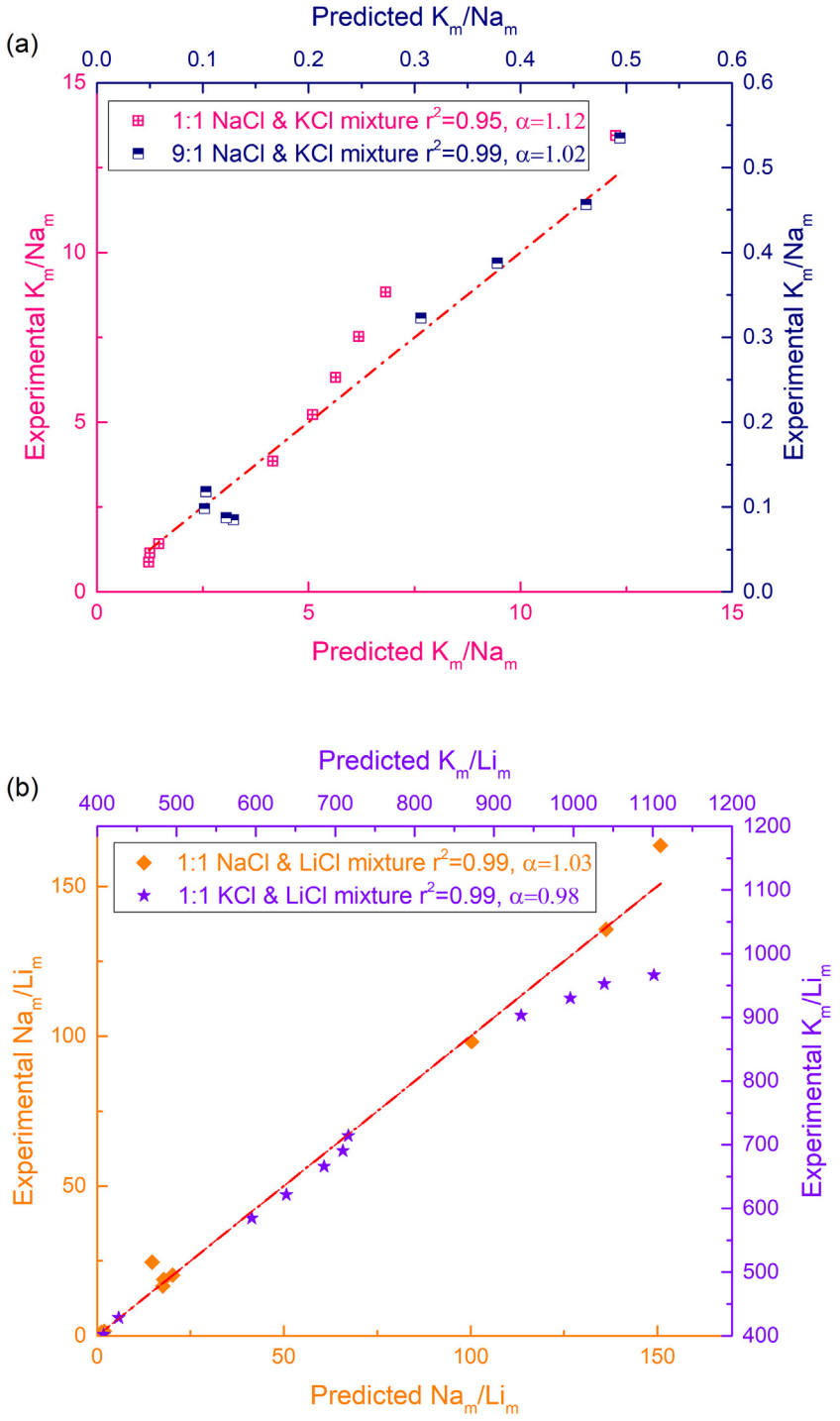

Fig. 6. Comparison between experimentally obtained and theoretically predicted membrane concentration ratios starting in symmetrical 1:1 and 9:1 NaCl:KCl solutions (a) or 1:1 KCl:LiCl and NaCl:LiCl solutions (b). The slope (α) and regression coefficient (r^2) for each data set (actual regression lines not shown) are indicated. The calculated α and r^2 values for the 1:1 KCl:LiCl solution is based on the linear part of the data set with $K_m/Li_m < 800$. The dotted line, added as visible guidance, represents the line of equality with $\alpha = 1$.

and Na^+ (Eqs. (16) & (17)) and ion partitioning (Eqs. (10) & (18)).

$$CE_{tot} = CE_0 + CE\text{-}K + CE\text{-}Na \quad (14)$$

$$A = K_m + Na_m + CE\text{-}K + CE\text{-}Na \quad (15)$$

$$CE\text{-}K = K_K \times K_m \times CE_0 \quad (16)$$

$$CE\text{-}Na = K_{Na} \times Na_m \times CE_0 \quad (17)$$

$$K_m = \alpha \times Na_m \times K_f/Na_f \quad (18)$$

Combining Eqs. (14)–(17) renders:

$$K_m + Na_m = A - \frac{CE_{tot} \times (K_K K_m + K_{Na} Na_m)}{1 + K_K K_m + K_{Na} Na_m} \quad (19)$$

Substitution of Eq. (18) in Eq. (19) results in an implicit expression for Na_m which can be solved for Na_m using, for instance, the Solver function in Excel, giving a unique solution independent of the starting value of Na_m. With CE covalently attached to the bulky siloxane-based polymer, the concentration of free Na^+ in the membrane is of particular

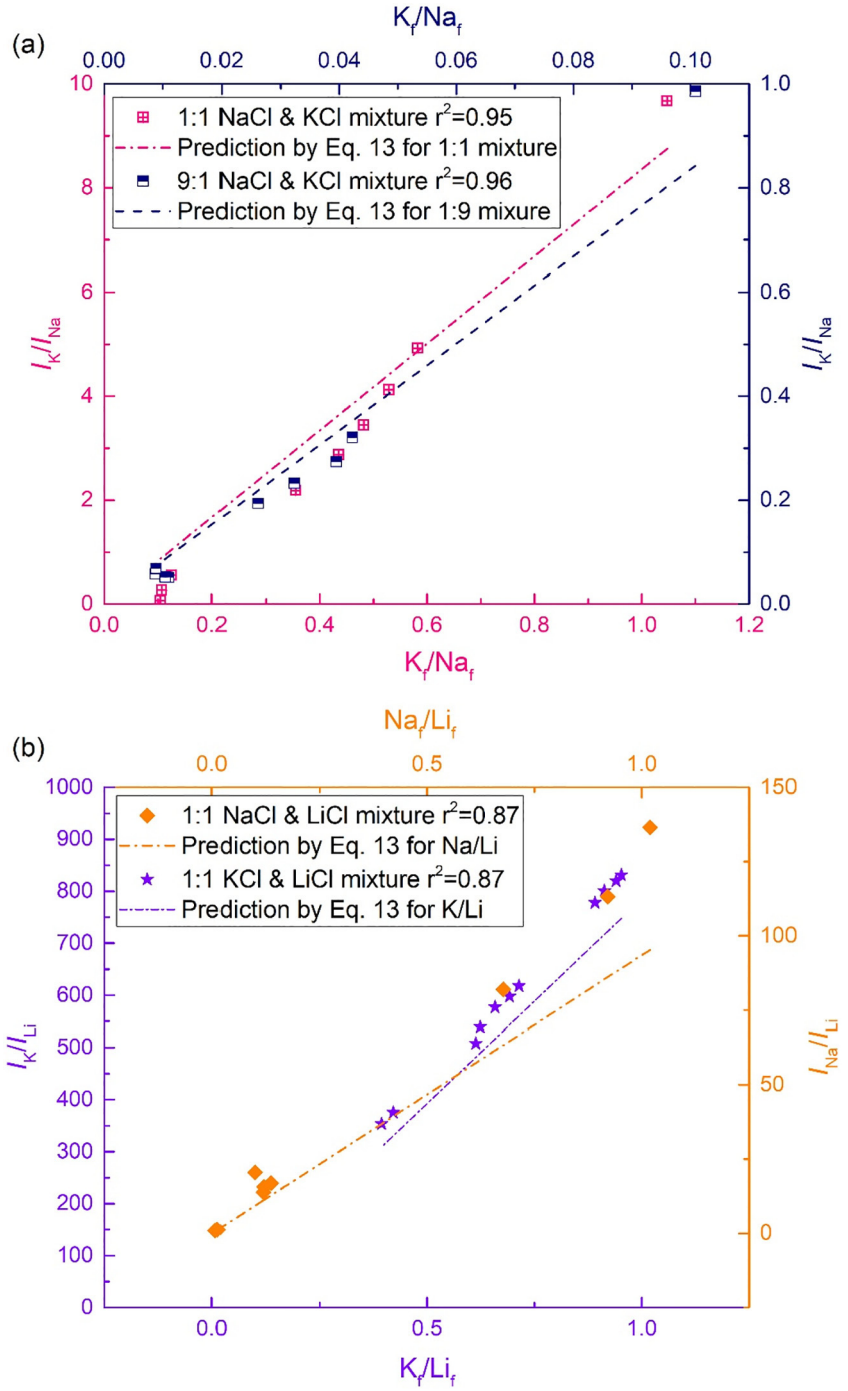

Fig. 7. Experimentally obtained current ratio plotted as function of the (time-dependent) feed concentration ratio. Dashed lines are based on theoretical values of β according to Eq. (13). Data based on recordings in symmetrical 1:1 or 9:1 NaCl:KCl solutions (a) or 1:1 KCl:LiCl and NaCl:LiCl solutions (b). The regression coefficient (r^2) for each data set (actual regression lines not shown) is indicated.

interest because this is the species responsible for the Na^+ carried current over the membrane. Fig. 8 plots the free Na^+ and K^+ concentrations as function of the ratio of the two equilibrium interaction constants K_K/K_{Na}, in symmetrical 1:1 (a) and asymmetrical 9:1 (Na^+:K^+) solutions. For an equimolar feed solution and with the affinity constants of CE-K and CE-Na set at 0.0025 M^{-1} and at a value < 0.001 M^{-1}, respectively (with K_K/K_{Na} > 25), the K^+ current reduction is around 30%, *i.e.* the reduction observed is in the single-salt KCl measurements in the presence of CE (Fig. 3). Increasing K_{Na} and decreasing K_K, resulting in K_K/K_{Na} = 0.01, strongly affects the free membrane concentration of both K^+ and Na^+; however, their ratio remains the same.

Given that ion partitioning occurs at a much faster time scale than complexation, this result is inherently hidden in the model. Fig. 7, showing a current ratio closely following the (time-dependent) feed concentration, both in 1:1 and 9:1 Na^+/K^+ solution, supports this view. If correct, this observation also implies that ion currents are exclusively carried by the free ion species in the membrane. In summary, for a (SLM) system as described in this study, in which the ion partitioning over the aqueous and membrane phase dictates the ratio of free K^+ and Na^+ concentrations in the membrane, the current ratio closely follows the concentration ratio in the feed solution.

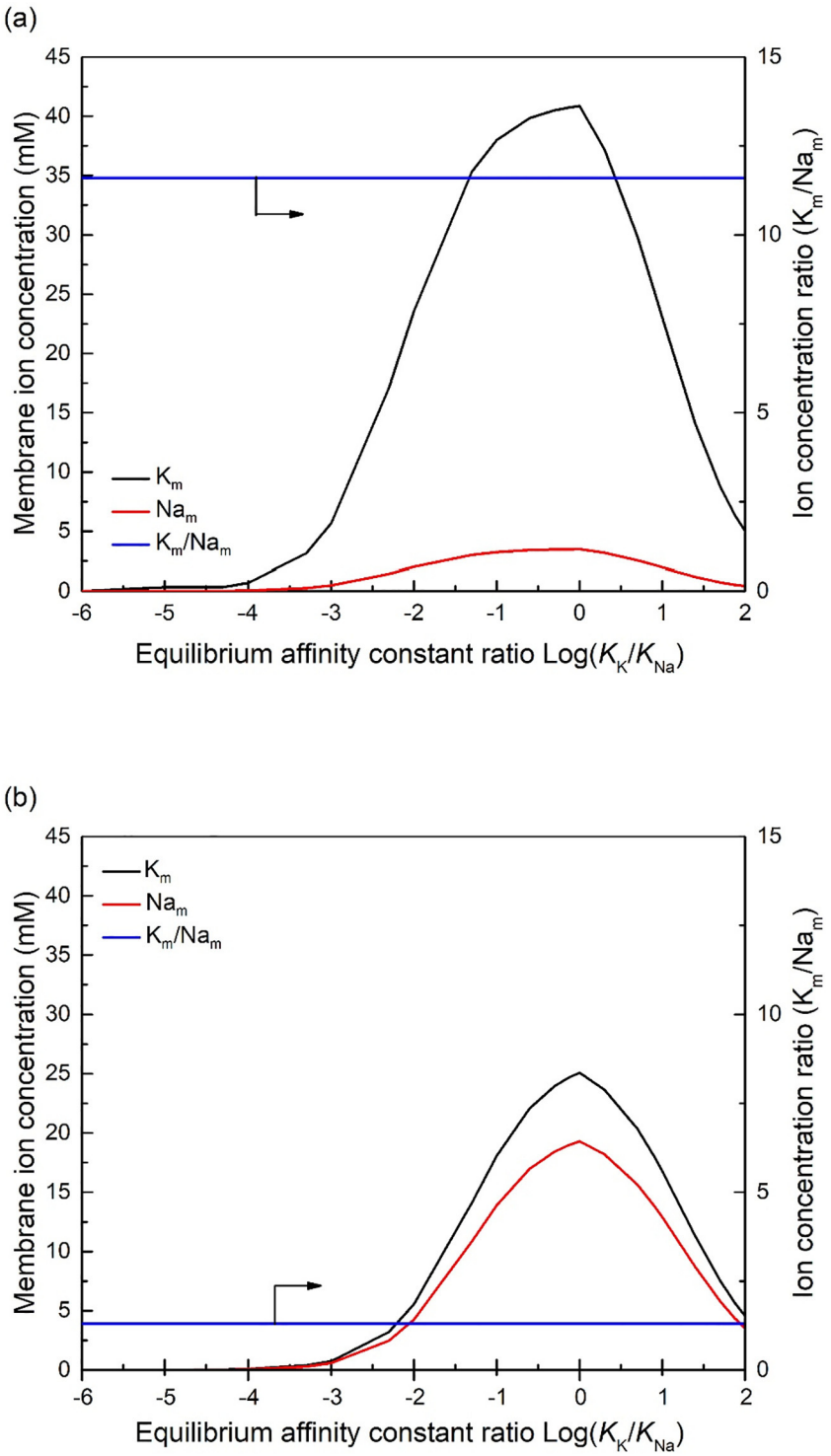

Fig. 8. Simulated free K^+ and Na^+ concentrations in the membrane (in mM) as function of the ratio of the (arbitrary set) equilibrium affinity constants K_K/K_{Na} in a feed solution of either 1:1 (a) or 9:1 (b) NaCl & KCl. The total amount of lipophilic anion and total amount of 15-crown-5 is 0.05 M and 0.13 M, respectively.

3.9. Implementation

A first requirement for implementation is membrane stability and longevity. Therefore, in addition to the morphology test as described in the Supplementary Information, a functionality test over time has been performed. To this end, the same ED experiment was repeated twice using the same SLM and fresh solutions each time. The K^+ over Na^+ separation efficiency, S(K/Na), was assessed in symmetrical solutions containing 0.05 M KCl and 0.05 M NaCl and under the same experimental conditions as described in the main text for the other ED experiments. Fig. 9 shows for each run the calculated S(K/Na) as a function of the normalized feed concentration ratio. Even though the curves not fully overlap, in both runs S(K/Na) follows the same trend with respect to the feed concentration ratio. Despite the observed shift, the loss in separation efficiency, as recorded over a total time period of 96 h, remains limited to 5–10%. Current investigations include strategies to further improve the SLM stability over time.

The conclusions drawn in previous paragraphs have implications for

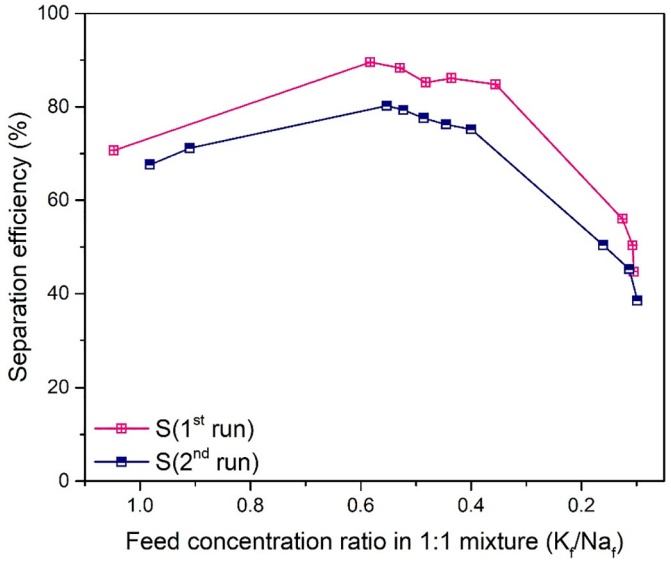

Fig. 9. Calculated K^+ over Na^+ separation efficiency of two ED experiments in series over a total time period of 96 h using the same membrane and fresh solutions each time and measured in symmetrical 0.05 M NaCl + 0.05 M KCl solutions.

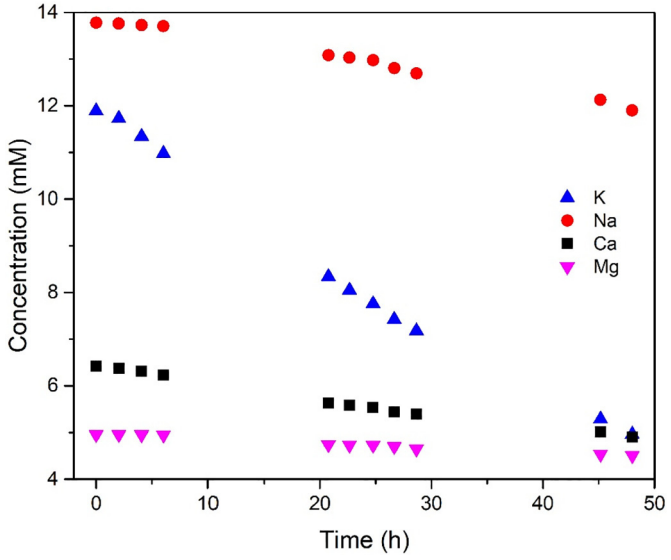

Fig. 10. K^+, Na^+, Ca^{2+}, Mg^{2+} concentrations changes over time in symmetrical synthetic drainage irrigation water.

the application we aim for, *i.e.*, the selective removal of Na^+ from the drainage water of greenhouses (major cations present are K^+, Na^+, Ca^{2+} and Mg^{2+}) and process design. Firstly, as can be concluded from Fig. 5, the K^+ over Na^+ separation efficiency can be optimized by controlling the feed concentration ratio within a certain range. Secondly, the Na^+/K^+ concentration ratio of the drainage water leaving the greenhouse typically is 1–1.5. As remarked, as long as Na^+/K^+ concentration ratio < 8.4 will K^+ be the dominant ion species to be removed. The actual drainage water leaving the greenhouse contains about the same concentration of K^+ and Na^+. Therefore, in order to extent our findings to the real-life situation, Fig. 10 shows the result of a preliminary ED experiment using a synthetic salt solution with, regarding the four most prominent cationic constituents, the same composition as natural drainage irrigation water: Na^+: 13.8 mM, K^+: 11.9 mM, Ca^{2+}: 6.4 mM and Mg^{2+}: 5 mM (data provided by Van der Knaap). As shown in Fig. 9, with more or less the same K^+ and Na^+ concentration (12–14 mM) and in the presence of Ca^{2+} and Mg^{2+}, K^+ transport clearly is favored by the SLM under ED conditions.

Consequently, the implementation of this technology for the intended greenhouse application of selectively removing Na^+ requires a two-step cleaning process. Fig. 11 schematically outlines two different process designs based on the use of two types of membranes, the SLM developed here and a standard monovalent over divalent cation selective membrane. In the first option, as shown in Fig. 11a using the SLM, K^+ is selectively removed first, followed by a second step which removes the remaining Na^+ from the retentate. The second option as shown in Fig. 11b starts out with the removal of both K^+ and Na^+, followed by the selective separation of K^+ from this permeate using the SLM. In both scenarios, afterwards the recovered K^+ is re-combined with the divalent cation-containing solution.

Finally, a brief comment on the economic feasibility of the technology outlined here. In a previous study of this lab this issue has been addressed [15]. However, in that entirely theoretical exercise we anticipated the mandatory inclusion of crown-ether in the SLM. The conclusion then was that the capital cost of the SLM was dominated by the price of crown-ether. Evidently, the experimental results shown in the present study point to the fact that an effective separation does not require the presence of crown ether. In the absence of crown ether, borate determines to a large extent the price of the SLM resulting in (an estimated) price per m^2 of 828 euro. This still is almost three times the price of a typical ion exchange membrane of Neosepta (300 euro per m^2; EURODIA, 2019). However, in order to achieve similar selectivity properties than described here for the SLM requires the Neosepta membrane to be chemically modified, which will force its price upwards. As for the operational costs of the SLM, notably the power consumption, the reader is referred to [15].

4. Final remarks

Studies reporting the efficient separation of a monovalent cation species from a solution containing other monovalent cation species as well remain scarce, even more so for (binary) K^+/Na^+ solutions. But based on what has been reported and to the best of our knowledge, the performance of the SLM system described here ranks rather high regarding its selectivity. For instance, using a dopamine-covered sulfonated polysulfone membrane resulted in K^+ over Li^+ selectivity of 2.9, as assessed under ED conditions [42]. A similar result, *i.e.*, a K^+ over Li^+ selectivity of 2.3 (also under ED conditions), was found when using a polyelectrolyte-coated Nafion membrane instead [34]. These numbers are rather modest compared to the K^+/Li^+ selectivity values shown in Fig. 7b, indeed even with the K^+/Na^+ selectivity shown in Fig. 7a (both at 1:1 feed concentrations). Adding a crown ether may enhance the selectivity properties of the system [43] but this often is at the expense ion mobility, resulting in higher membrane resistances [42]. Interestingly, Guo and co-workers report on a rather high discrimination between K^+ and Li^+ applying a polymer/metal-organic framework composite [44]. However, the Li^+ over Na^+/K^+ selectivity of 35–67 reflects an inversed selectivity in which the smallest ion species is favored, thereby pointing to a selectivity mechanism based on sieving rather than partitioning.

The SLM system described here shows a permeation preference for the ionic species with the largest crystal radius ($K^+ > Na^+ > Li^+$) with, by definition, the lowest dehydration energy. To quantify dehydration, the Born equation was used instead of the Gibbs free energy of dehydration. The reason is that in our case, describing ion transfer from water into NPOE, the Born approach is more realistic as the standard Gibbs free energy of dehydration refers to the transfer from water to vacuum (see also Luo et al.) [10]. As argued, the ion radius plays a key role in the behavior of the SLM, as expressed by Eq. 13 and shown in Fig. 7. Even though reported crystal radii slightly vary (*e.g.* Atkins et al. [45] lists Na^+ and K^+ radii of 1.02 Å and 1.38 Å, respectively), those differences do not affect the overall observed trends in the membrane

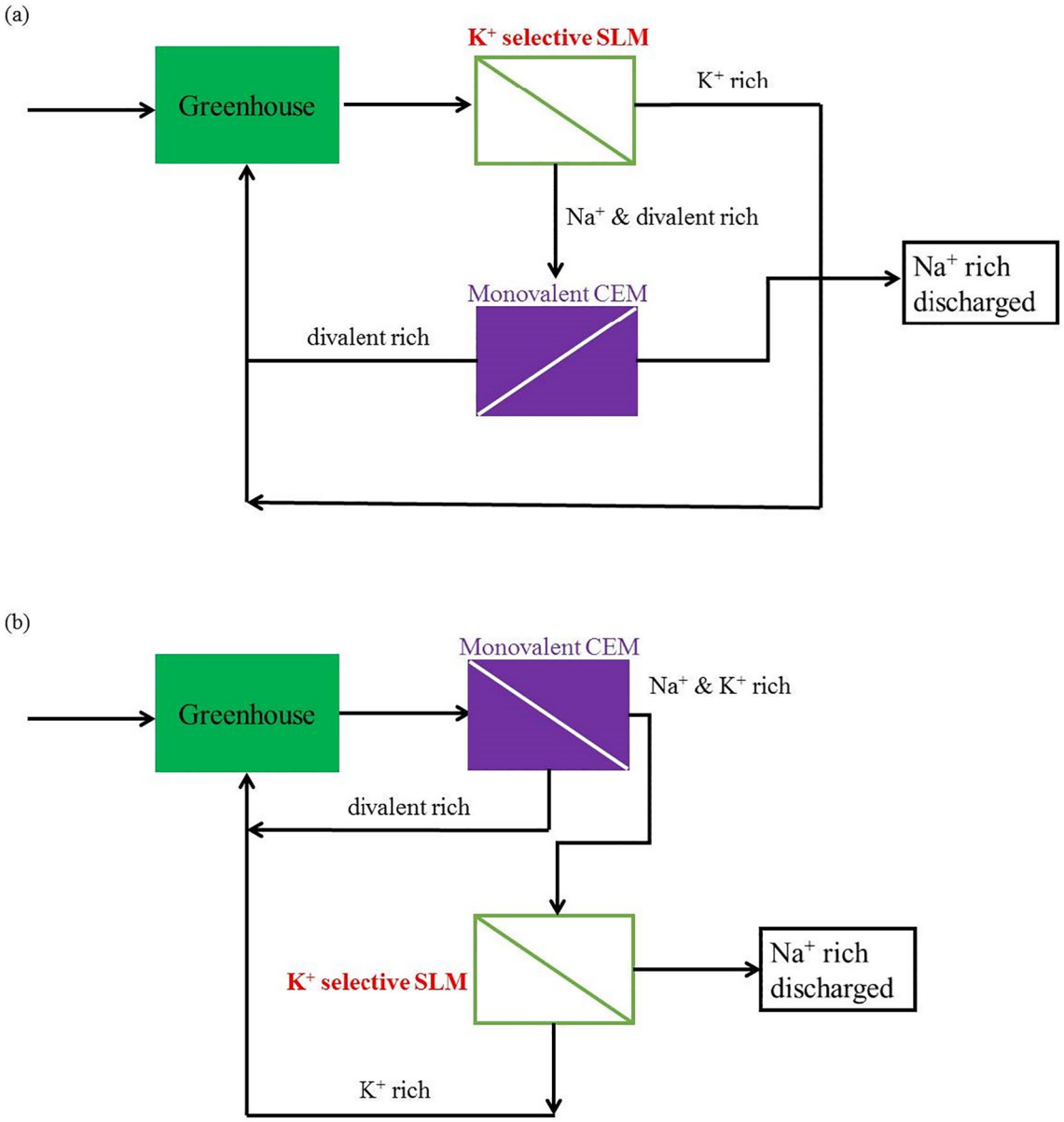

Fig. 11. Two different process designs for the removal of excess Na^+ from (circulated) greenhouse drainage water. Both two-step processes are based on the use of the SLM developed here and a membrane with a monovalent over divalent cation selectivity.

separation performance.

As shown, the calculated mobility ratio of two ion species in the SLM is directly proportional to the inverse ratio of both crystal radii, in the same way as the mobility ratio in water relates to the ratio of the (hydrated) Stokes radius of the two ion species. Despite this relationship, the calculated absolute mobility values are an order of two smaller than those measured in water, despite their smaller radius. One explanation is that the permeating cation (somehow) interacts with NPOE, for example, *via* cation-π interaction or, alternatively, interacts with the lipophilic anions dissolved in NPOE [46]. In addition, the higher viscosity of NPOE (13.8 mPa.s *versus* 0.89 mPa.s of water) [47,48] may impede ion movement.

Regarding a possible interaction between the permeant cation and the lipophilic anion, given the borate concentration of 0.05 M, the average distance between two borate sites is 3.2 nm. Apparently, the (temporal) interaction between the cation and the borate anion slows down the overall mobility but the mobility required to jump (or hop) from one site to another still is inversely proportional to the crystal radius of the ion. As remarked before, such cation – borate interaction could (partly) explain the deviation of SLM behavior from theoretical prediction (Fig. 7). The relatively low borate concentration of 0.05 M is related to the observed relatively high SLM resistance. Even though the addition of borate to the NPOE significantly decreases the membrane resistance and transforms the SLM into a highly cation selective membrane, the resistance still is relatively high compared to that of existing commercially available ion-exchange membranes, typically 1–2 Ω cm^{-2}. The reason for the high resistance of the SLM reflects its limited ion-exchange capacity (IEC) of 0.05 M, compared to 1 M for typical ion exchange membranes. As remarked already, ions may move through the membrane by hopping from borate site to borate site, with these sites located 3.2 nm apart from each other. A prerequisite of such hopping mechanism is a high enough borate density and by implication a not too large mutual distance between adjacent sites. The percolation theory provides a theoretical frame work of this concept. Tongwen et al. [49], presented a general percolation model applicable to all kinds of ionomeric systems. Only when the IEC exceeds a certain threshold value are conductive channels formed allowing an effective flow of ions. The (generic) IEC threshold reported Tongwen et al. ranges from

0.54 to 1.07 mEq per gram dry membrane. Assuming a zero water content of our SLM, the 0.05 M borate applied translates to an IEC value of 0.068 mEq per gram of NPOE/membrane, at least almost a factor 10 lower than the abovementioned value. This may indeed (partly) explain the high resistance observed. Unfortunately, the applied 0.05 M lipophilic borate represents already the maximal solubility of NaBArF in NPOE, hampering us to test our hypothesis by increasing the borate concentration.

Lastly, regarding the relatively lower resistances of other membrane systems, one should bear in mind that the (efficient) transport of one particular ion species and ion selectivity are two related but nevertheless different issues. For instance, ceramic NASICON-based membranes show high Na^+ transport rates but only in the absence of K^+ [50–52]. Evidently, under free K^+ conditions there is no need for a high Na^+ over K^+ membrane selectivity. The same holds for all types of Li^+ selective membrane as applied in lithium battery technology where Li^+ is the only monovalent cation present [51]. As soon as selectivity is required, one encounters the frequently reported trade-off seen in membrane transport studies in which increased selectivity pairs with decreased flux and *vice versa* [53,54].

5. Conclusions

This study shows the ability to separate two ion species that are very similar regarding charge and size. The novel aspect of the present study is, firstly, the high separation efficiency (up to ~90% for K^+ over Na^+ to ~100% for K^+ over Li^+) and, secondly, that achieving such high separation does not require the presence of carrier molecules in the membrane. Essentially, the working mechanism of the supported liquid membrane used comes back entirely to the radii of the two ion species involved. Entering the hydrophobic NPOE containing membrane (permittivity = 24) requires the ions to be (partly) dehydrated. According to the Born equation, the larger the crystal ion radius, the lower this dehydration energy. The partitioning ratio in turn, dictated by Boltzmann distributions, scales exponentially with the difference in dehydration energy. The lower mobility of the largest ion species in the SLM cannot compensate for this dehydration/partitioning effect, consequently the SLM favors the largest ion species. Together with the concentration ratio in the feed solution, these basic physico-chemical principles suffice to adequately describe the behavior of the SLM.

Author statement

Zexin Qian: Conceptualization, Investigation, Formal analysis, Data curation, Writing - original draft. **Henk Miedema**: Supervision, Conceptualization, Formal analysis, Data curation, Writing - review & editing. **Sevil Sahin**: Investigation, Data curation (synthesis part). **Louis C.P.M. de Smet**: Supervision, Formal analysis, Writing - review & editing. **Ernst J.R. Sudhölter**: Supervision, Conceptualization, Writing - review & editing.

Declaration of competing interest

The authors declare that they have no known competing financial interests or personal relationships that could have appeared to influence the work reported in this paper.

Acknowledgements

This work was performed in the cooperation framework of Wetsus, European Centre of Excellence for Sustainable Water Technology (www.wetsus.nl). Wetsus is co-funded by the Dutch Ministry of Economic Affairs and Ministry of Infrastructure and Environment, the European Union Regional Development Fund, the Province of Fryslan and the Northern Netherlands Provinces. This work is part of a project that has received funding from the European Union's Horizon 2020 research and innovation program under the Marie Skfodowska-Curie grant agreement No 65874. The authors like to thank the participants of the research theme “Desalination” for the fruitful discussions and their financial support. A special word of thank goes to Van der Knaap (The Netherlands) and Yara (The Netherlands) for all their advice and support. L.C.P.M.d.S. acknowledges the European Research Council (ERC) for a Consolidator Grant, which is part of the European Union's Horizon 2020 research and innovation program (grant agreement No. 682444).

Appendix A. Supplementary data

Supplementary data to this article can be found online at https://doi.org/10.1016/j.desal.2020.114631.

References

[1] M. Sadrzadeh, T. Mohammadi, Sea water desalination using electrodialysis, Desalination. 221 (2008) 440–447, https://doi.org/10.1016/J.DESAL.2007.01.103.
[2] A.H. Galama, M. Saakes, H. Bruning, H.H.M. Rijnaarts, J.W. Post, Seawater predesalination with electrodialysis, Desalination. 342 (2014) 61–69, https://doi.org/10.1016/j.desal.2013.07.012.
[3] T. Chakrabarty, A.M. Rajesh, A. Jasti, A.K. Thakur, A.K. Singh, S. Prakash, V. Kulshrestha, V.K. Shahi, Stable ion-exchange membranes for water desalination by electrodialysis, Desalination. 282 (2011) 2–8, https://doi.org/10.1016/j.desal.2011.08.009.
[4] H. Strathmann, Electrodialysis, a mature technology with a multitude of new applications, Desalination. 264 (2010) 268–288, https://doi.org/10.1016/j.desal.2010.04.069.
[5] Y. Tanaka, Ion-exchange membrane electrodialysis program and its application to multi-stage continuous saline water desalination, Desalination. 301 (2012) 10–25, https://doi.org/10.1016/j.desal.2012.06.007.
[6] G.J. Doornbusch, M. Tedesco, J.W. Post, Z. Borneman, K. Nijmeijer, Experimental investigation of multistage electrodialysis for seawater desalination, Desalination. 464 (2019) 105–114, https://doi.org/10.1016/j.desal.2019.04.025.
[7] M. Mulder, Basic Principles of Membrane Technology, 2nd ed., Springer, Netherlands, Dordrecht, 1996, https://doi.org/10.1007/978-94-009-1766-8_1.
[8] H. Strathmann, Membrane separation processes, J. Memb. Sci. 9 (1981) 121–189, https://doi.org/10.1016/S0376-7388(00)85121-2.
[9] H. Strathmann, Ion-exchange Membrane Separation Processes, Elsevier, Amsterdam, 2004, https://doi.org/10.1007/s13398-014-0173-7.2.
[10] T. Luo, S. Abdu, M. Wessling, Selectivity of ion exchange membranes: a review, J. Memb. Sci. 555 (2018) 429–454, https://doi.org/10.1016/j.memsci.2018.03.051.
[11] M. Irfan, Y. Wang, T. Xu, Novel electrodialysis membranes with hydrophobic alkyl spacers and zwitterion structure enable high monovalent/divalent cation selectivity, Chem. Eng. J. (2019), https://doi.org/10.1016/j.cej.2019.123171.
[12] S. Caprarescu, M.C. Corobea, V. Purcar, C.I. Spataru, R. Ianchis, G. Vasilievici, Z. Vuluga, San copolymer membranes with ion exchangers for Cu(II) removal from synthetic wastewater by electrodialysis, J. Environ. Sci. (China) 35 (2015) 27–37, https://doi.org/10.1016/j.jes.2015.02.005.
[13] S. Caprarescu, A.L. Radu, V. Purcar, A. Sarbu, D.I. Vaireanu, R. Ianchis, M. Ghiurea, Removal of copper ions from simulated wastewaters using different bicomponent polymer membranes, Water Air Soil Pollut. 225 (2014) 1–12, https://doi.org/10.1007/s11270-014-2079-6.
[14] C.Y. Foong, M.D.H. Wirzal, M.A. Bustam, A review on nanofibers membrane with amino-based ionic liquid for heavy metal removal, J. Mol. Liq. 297 (2020) 111793, , https://doi.org/10.1016/j.molliq.2019.111793.
[15] Z. Qian, H. Miedema, L.C.P.M. de Smet, E.J.R. Sudhölter, Modelling the selective removal of sodium ions from greenhouse irrigation water using membrane technology, Chem. Eng. Res. Des. 134 (2018) 154–161, https://doi.org/10.1016/j.cherd.2018.03.040.
[16] F.J.M. Maathuis, A. Amtmann, K+ nutrition and Na+ toxicity: the basis of cellular K+/Na+ ratios, Ann. Bot. 84 (1999) 123–133, https://doi.org/10.1006/anbo.1999.0912.
[17] E. Blumwald, Sodium transport and salt tolerance in plants, Curr. Opin. Cell Biol. 12 (2000) 431–434, https://doi.org/10.1016/S0955-0674(00)00112-5.
[18] J.L. Zhang, T.J. Flowers, S.M. Wang, Mechanisms of sodium uptake by roots of higher plants, Plant Soil 326 (2010) 45–60, https://doi.org/10.1007/s11104-009-0076-0.
[19] J. Bobacka, A. Ivaska, A. Lewenstam, Potentiometric ion sensors, Chem. Rev. 108 (2008) 329–351, https://doi.org/10.1021/cr068100w.
[20] T. Guinovart, D. Hernández-Alonso, L. Adriaenssens, P. Blondeau, F.X. Rius, P. Ballester, F.J. Andrade, Characterization of a new ionophore-based ion-selective electrode for the potentiometric determination of creatinine in urine, Biosens. Bioelectron. 87 (2017) 587–592, https://doi.org/10.1016/j.bios.2016.08.025.
[21] N.M. Kocherginsky, Q. Yang, L. Seelam, Recent advances in supported liquid membrane technology, Sep. Purif. Technol. 53 (2007) 171–177, https://doi.org/10.1016/j.seppur.2006.06.022.
[22] P.K. Parhi, Supported liquid membrane principle and its practices: a short review, J.

Chem. 2013 (2013) 1–11, https://doi.org/10.1155/2013/618236.
[23] R.A. Bartsch, J.D. Way, Chemical Separations with Liquid Membranes: an Overview, (1996), pp. 1–10, https://doi.org/10.1021/bk-1996-0642.ch001.
[24] M.M. Naim, A.A. Monir, Desalination using supported liquid membranes, Desalination. 153 (2003) 361–369, https://doi.org/10.1016/S0011-9164(02)01129-3.
[25] T. Rosatzin, E. Bakker, K. Suzuki, W. Simon, Lipophilic and immobilized anionic additives in solvent polymeric membranes of cation-selective chemical sensors, Anal. Chim. Acta 280 (1993) 197–208, https://doi.org/10.1016/0003-2670(93)85122-Z.
[26] E. Bakker, E. Pretsch, Lipophilicity of tetraphenylborate derivatives as anionic sites in neutral carrier-based solvent polymeric membranes and lifetime of corresponding ion-selective electrochemical and optical sensors, Anal. Chim. Acta 309 (1995) 7–17, https://doi.org/10.1016/0003-2670(95)00077-D.
[27] F.G. Bănică, Chemical Sensors and Biosensors: Fundamentals and Applications, John Wiley and Sons, Chichester, UK, 2012, https://doi.org/10.1002/9781118354162.
[28] W. Walkowiak, C.A. Kozlowski, Macrocycle carriers for separation of metal ions in liquid membrane processes-a review, Desalination. 240 (2009) 186–197, https://doi.org/10.1016/j.desal.2007.12.041.
[29] M.M. Wienk, T.B. Stolwijk, E.J.R. Sudhölter, D.N. Reinhoudt, Stabilization of crown ether containing supported liquid membranes, J. Am. Chem. Soc. 112 (1990) 797–801, https://doi.org/10.1021/ja00158a046.
[30] A. Šlampová, P. Kubáň, P. Boček, Fine-tuning of electromembrane extraction selectivity using 18-crown-6 ethers as supported liquid membrane modifiers, Electrophoresis. 35 (2014) 3317–3320, https://doi.org/10.1002/elps.201400372.
[31] A. Oberta, J. Wasilewski, R. Wódzki, Selective lead(II) transport in a liquid membrane system with octylsulfanylacetic acid ionophore, Desalination. 252 (2010) 40–45, https://doi.org/10.1016/j.desal.2009.11.004.
[32] P. Długołecki, K. Nymeijer, S. Metz, M. Wessling, Current status of ion exchange membranes for power generation from salinity gradients, J. Memb. Sci. 319 (2008) 214–222, https://doi.org/10.1016/j.memsci.2008.03.037.
[33] J.A. Ibáñez-Mengual, J. García-Gamuz, R.P. Valerdi-Pérez, Bi-ionic potential: experimental measurements and diffusion coefficients determinations, Desalin. Water Treat. 36 (2011) 81–88, https://doi.org/10.5004/dwt.2011.2072.
[34] L. Yang, C. Tang, M. Ahmad, A. Yaroshchuk, M.L. Bruening, High selectivities among monovalent cations in dialysis through cation-exchange membranes coated with polyelectrolyte multilayers, ACS Appl. Mater. Interfaces 10 (2018) 44134–44143, https://doi.org/10.1021/acsami.8b16434.
[35] A. Kumar, P.S.H. Rizvi, A.M.S. Requena, Handbook of Membrane Separations: Chemical, Pharmaceutical, Food, and Biotechnological Applications, 2nd ed., CRC Press, 2015.
[36] E.R. Nightingale, Phenomenological theory of ion solvation. Effective radii of hydrated ions, J. Phys. Chem. 63 (1959) 1381–1387, https://doi.org/10.1021/j150579a011.
[37] R.A. Robinson, R.H. Stokes, Electrolyte Solutions: Second Revised Edition, Dover Publications, 2002.
[38] B. Van Der Bruggen, A. Koninckx, C. Vandecasteele, Separation of monovalent and divalent ions from aqueous solution by electrodialysis and nanofiltration, Water Res. 38 (2004) 1347–1353, https://doi.org/10.1016/j.watres.2003.11.008.
[39] L. Torun, New Crown Ether Compounds and their Alkali Metal Ion Complexation, (1994).
[40] Y. Liu, L.H. Tong, S. Huang, B.Z. Tian, Y. Inoue, T. Hakushi, Complexation thermodynamics of bis(crown ether)s. 4. Calorimetric titration of intramolecular sandwich complexation of thallium and sodium ions with bis(15-crown-5)s and bis(12-crown-4)s: enthalpy-entropy compensation, J. Phys. Chem. 94 (1990) 2666–2670, https://doi.org/10.1021/j100369a079.
[41] J. Kim, M. Shamsipur, S.Z. Huang, R.H. Huang, J.L. Dye, Sandwich and mixed sandwich complexes of the cesium ion with crown ethers in nitromethane, J. Phys. Chem. A 103 (1999) 5615–5620, https://doi.org/10.1021/jp990685t.
[42] S. Yang, Y. Liu, J. Liao, H. Liu, Y. Jiang, B. Van Der Bruggen, J. Shen, C. Gao, Codeposition modification of cation exchange membranes with dopamine and crown ether to achieve high K+ electrodialysis selectivity, ACS Appl. Mater. Interfaces 11 (2019) 17730–17741, https://doi.org/10.1021/acsami.8b21031.
[43] S. Chaudhury, A. Bhattacharyya, A. Goswami, Electrodriven ion transport through crown ether–nafion composite membrane: enhanced selectivity of Cs^{+} over Na^{+} by ion gating at the surface, Ind. Eng. Chem. Res. 53 (2014) 8804–8809, https://doi.org/10.1021/ie500934v.
[44] Y. Guo, Y. Ying, Y. Mao, X. Peng, B. Chen, Polystyrene sulfonate threaded through a metal-organic framework membrane for fast and selective lithium-ion separation, Angew. Chemie Int. Ed. 55 (2016) 15120–15124, https://doi.org/10.1002/anie.201607329.
[45] P. Atkins, T. Overton, J. Rourke, M. Weller, F. Armstrong, Shriver and Atkins' Inorganic Chemistry, Oxford University Press, 2009, http://www.amazon.co.uk/Shriver-Atkins-Inorganic-Chemistry-Peter/dp/0199236178.
[46] C. Miller, Ionic hopping defended, J. Gen. Physiol. 113 (1999) 783–787, https://doi.org/10.1085/jgp.113.6.783.
[47] Z. Samec, J. Langmaier, A. Trojánek, E. Samcová, J.Í. Málek, J. Heyrovskiýinstituteheyrovský, Transfer of Protonated Anesthetics Across the Water|O-Nitrophenyl Octyl Ether Interface: Effect of the Ion Structure on the Transfer Kinetics and Pharmacological Activity, (1998).
[48] J.C. Crittenden, R.R. Trussell, D.W. Hand, K.J. Howe, G. Tchobanoglous, MWH's Water Treatment: Principles and Design: Third Edition, John Wiley and Sons, 2012, https://doi.org/10.1002/9781118131473.
[49] X. Tongwen, Y. Weihua, H. Binglin, Ionic conductivity threshold in sulfonated poly (phenylene oxide) matrices: a combination of three-phase model and percolation theory, Chem. Eng. Sci. 56 (2001) 5343–5350, https://doi.org/10.1016/S0009-2509(01)00242-1.
[50] J. Bartrolí, L. Alerm, P. Fabry, E. Siebert, Conductive epoxy-graphite composite as a solid internal reference in a NASICON-based sodium ion-selective electrode for flow-injection analysis, Anal. Chim. Acta 308 (1995) 102–108, https://doi.org/10.1016/0003-2670(94)00655-6.
[51] M. Cretin, P. Fabry, Comparative study of lithium ion conductors in the system Li1 + xAlxA2-xIV (PO4)3 with AIV = Ti or Ge and $0 \leq x \leq 0{\cdot}7$ for use as Li+ sensitive membranes, J. Eur. Ceram. Soc. 19 (1999) 2931–2940, https://doi.org/10.1016/s0955-2219(99)00055-2.
[52] S. Balagopal, T. Landro, S. Zecevic, D. Sutija, S. Elangovan, A. Khandkar, Selective sodium removal from aqueous waste streams with NaSICON ceramics, Sep. Purif. Technol. 15 (1999) 231–237, https://doi.org/10.1016/S1383-5866(98)00104-X.
[53] H.B. Park, J. Kamcev, L.M. Robeson, M. Elimelech, B.D. Freeman, Maximizing the right stuff: The trade-off between membrane permeability and selectivity, Science 356 (2017) 1138–1148, https://doi.org/10.1126/science.aab0530 (80-.).
[54] B.D. Freeman, Basis of permeability/selectivity trade-off relations in polymeric gas separation membranes, Macromolecules. 32 (1999) 375–380, https://doi.org/10.1021/ma9814548.